Modeling of Feeding Behavior of Solidifying Al-7Si-0.3Mg Alloy Plate Casting

Y.W. LEE, E. CHANG, and C.F. CHIEU

The systematic change of riser size, together with the variation of geometries of solidifying Al-7Si-0.3Mg plate castings, was tested by thermal analysis to model the interdendritic feeding behavior based on Darcy's law. This law, however, is found to be only applicable to certain thermal conditions in the solidifying casting. The applicability of Darcy's law depends on the regime of solidification time. A new feeding efficiency parameter integrating all individual thermal variables, denoted as $(G \cdot t^{2/3})/V_s$ (where G is the thermal gradient, t is local solidification time, and V_s is solidus velocity), is found satisfactory to predict the formation of porosity. The combined geometries of a casting and its riser size exert a great influence on the thermal variables of Al-7Si-0.3Mg alloy in a complicated way. Together, these thermal variables synergize to govern the feeding behavior of the casting.

I. INTRODUCTION

THE formation of porosity in aluminum alloy is well known as a problem relating to its good thermal conductivity, long freezing range, and large decrease of hydrogen solubility from liquid state to solid state. This inevitable casting defect greatly deteriorates the soundness of casting. As such, numerous efforts have been carried out in an attempt to understand the feeding process of aluminum alloy by thermal measurement and to explore its feeding behavior by numerical analysis.

The importance of interdendritic fluid flow for the pore formation in solidification was pioneered by Piwonka and Flemings[1] and later by other investigators.[2–8] Davies[9] derived an equation which involves solidus velocity to calculate the capillary feeding distance for plate castings according to the Hagen-Poiseuill equation; however, the structural effect of the dendritic network was ignored. Niyama *et al.*[10] and later Minakawa *et al.*,[11] working on steel, postulated the same parameter $G/\sqrt{R}$, the thermal gradient divided by the square root of cooling rate, based on Darcy's law; the parameter verified that shrinkage decreased with increasing solidification time. The basis of this result is rationalized as the permeability of the dendritic network for capillary fluid flow increasing with increasing dendrite arm spacing which is proportional to solidification time.[4,7] Lecomte-Beckers[12] took into consideration alloying elements in a superalloy and proposed a microporosity index also based on Darcy's law; in essence, this work agrees with the previous work of Davies,[9] Niyama *et al.*,[10] and Minakawa *et al.*[11]

On the contrary, Poirier *et al.*,[13] in modeling the feeding behavior of Al-4.5 pct Cu, found that the porosity content decreased with increasing solidification rate and thermal gradient because of the smaller interdendritic spaces. In studying the same alloy, a similar conclusion was reached by Kubo and Pehlke,[14] although the latter authors also considered Darcy's law which governs the interdendritic fluid flow through porous media. This school of thinking was further supported by Entwistle *et al.*,[15] who evidenced the parallel relationship between porosity content and local solidification time for aluminum alloys.

In an attempt to reconcile the disagreement, Pathak and Prabhakar[16] postulated for aluminum alloys that the feeding efficiency is determined by both the pasty zone factor, feeding efficiency as influenced by pasty zone (FEP), and the interdendritic feeding time, feeding efficiency as influenced by the time allowed during the last stage of solidification (FET). However, contradiction exists as these two so-defined parameters, *i.e.*, FEP and FET, cannot be satisfied simultaneously; if the solidification rate is increased to improve the FEP, the FET will be sacrificed and *vice versa*. The dilemma was also noticed by Bachelet and Lesoult[17] in studying a superalloy, but no solution was attempted.

One of the reasons for failure to solve the above disputes, from the present authors' view, is that little attention is paid to the leeway of changing thermal conditions by larger variations in casting geometries. In this paper, the systematic change of riser size together with the variation of geometries of solidifying Al-7Si-0.3Mg plate castings were tested by thermal analysis to model the interdendritic feeding behavior based on Darcy's law. A new parameter that integrates thermal gradient, solidification time, and solidus velocity is derived to quantify the porosity formation of Al-7Si-0.3Mg aluminum alloy. More significantly, it is found that the applicability of Darcy's law depends on the regime of solidification time; thus, the disputes can be solved.

II. EXPERIMENTAL PROCEDURE

Rectangular plate castings were used in this experiment. The plates were 2-cm thick, 14-cm wide, and 15- or 25-cm long, with different riser sizes ranging from 4 to 11 cm in diameter. Table I exhibits the combinations studied in this experiment. Each combination of riser size and casting length for a proceeding casting was denoted

Y.W. LEE, Doctoral Candidate, and E. CHANG, Associate Professor, are with the Department of Materials Engineering, National Cheng Kung University, Tainan, Taiwan 70101, Republic of China. C.F. CHIEU, Foundry Engineer, is with the Materials Research Laboratories, Industrial Technology Research Institute, Hsinchu, Taiwan, Republic of China.

Manuscript submitted October 25, 1989.

Table I. Combination of Riser Sizes and Casting Lengths Studied

Casting Length (cm)	Riser Diameter (cm)					
15/25	4	5	6	7	8	11

as *D-L* (Figure 1), where *D* was the diameter of riser and *L* was the length of casting.

CO_2 molds were prepared using silica sand of AFS No. 100 and 7 wt pct sodium silicate as a binder. Thermocouples for thermal analysis were introduced into the center of the mold cavity along the longitudinal axis from free end to riser end at an equal interval and also into the riser center for obtaining cooling curves of castings, as shown in Figure 1. The molds were baked at 120 °C for 15 hours to exclude remaining water and cooled to ambient temperature before pouring. The melting process was performed in an electric resistance furnace, in which an Al-7Si-0.3Mg ingot was directly melted in a graphite crucible and degassed by moisture-free nitrogen to control the hydrogen content below 0.01 $cm^3/100$ g by reduced pressure test. When the temperature of the melt reached 720 °C, 0.5 wt pct Al-5Ti-1B was added. The pouring temperature was controlled at 700 °C ± 5 °C, and care was taken when filling the pouring basin to ensure steady and smooth flow of the melt.

The locations of the test pieces for density measurement and X-ray radiography are shown in Figure 2. The 3-mm-thick center slice was used for X-ray microradiography, and the 8 × 10 × 25-mm center rectangular blocks were used for density testing by Archimede's method. A cylindrical test casting chilled by copper disk and sufficiently fed by the riser (Figure 3) was also cast as a standard specimen with full density and was assumed to be free of porosity. Thus, the variation of porosity content longitudinally from free end to riser can be calculated.

III. THEORETICAL MODEL OF INTERDENDRITIC FEEDING

A. *Local Pressure at Interdendritic Feeding Channel*

It is believed that the mass feeding for a long freezing range alloy proceeds up to about 70 pct solidified melt before interdendritic feeding prevails, owing to pileup of

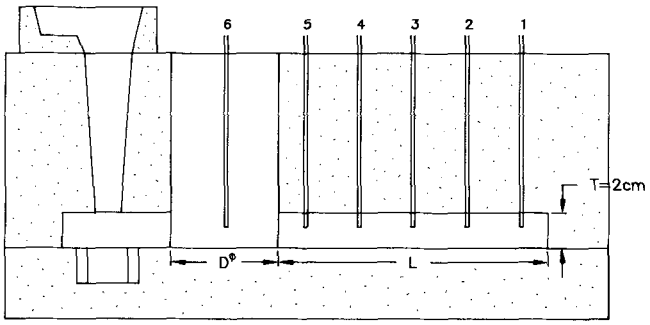

Fig. 1—Nomenclature of castings and arrangement of thermocouples in an assembled mold.

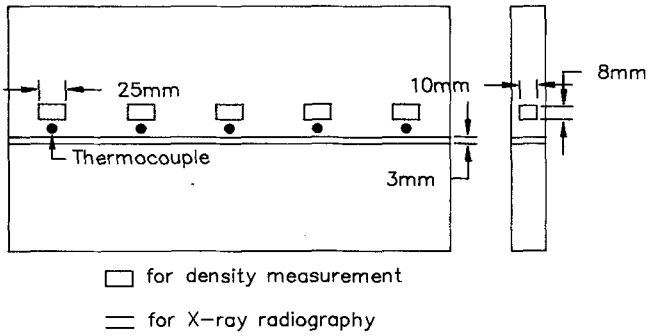

Fig. 2—Locations of test pieces for X-ray radiography and density measurement.

dendritic grains which form a three-dimensional network.[9] Interdendritic fluid flow becomes difficult as a consequence of the narrowing of the feeding channel by growth of the dendrite. The interference to fluid flow results in raising of the negative pressure at the dendrite root. The partially solidified long freezing range casting can be considered as a porous material; the corresponding interdendritic fluid flow through the porous material is suggested to be

$$V_L - V_s = \beta V_s = -\frac{K}{\mu f_L}(-\nabla P + \rho_L g) \qquad [1]$$

where V_L = liquidus velocity, $m \cdot s^{-1}$;
V_s = solidus velocity, $m \cdot s^{-1}$;
β = solidification shrinkage, pct;
K = permeability of porous material, m^2;
μ = viscosity of liquid, $N \cdot s \cdot m^{-2}$;
f_L = liquid fraction, pct;
P = local pressure in the fluid, $N \cdot m^{-2}$;
ρ_L = density of liquid, $kg \cdot m^{-3}$; and
g = acceleration of gravity, $m \cdot s^{-2}$

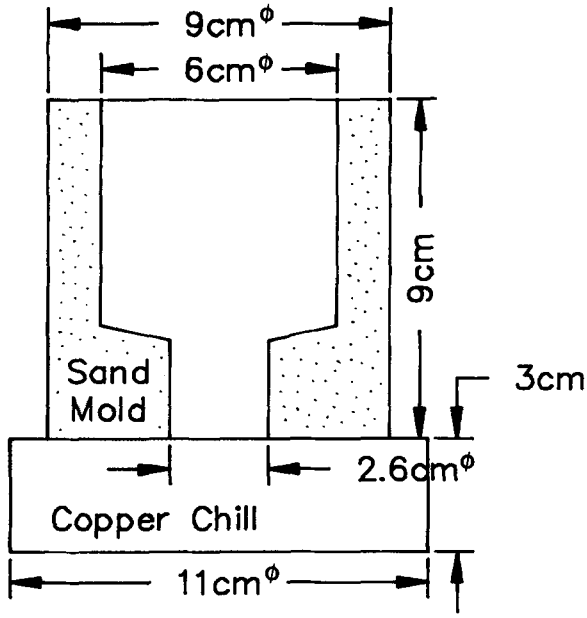

Fig. 3—Dimensioning of casting as a standard for the porosity measurement.

The permeability, K, and liquid fraction, f_L, are both functions of position. The x coordinate, as defined in Figure 4, where $x = 0$, is measured from the mass/interdendritic feeding interface. The permeability is generally accepted as $K = \gamma f_L^2(x)$, where γ is a variable depending on the structure of dendrite and the dendrite arm spacing. The local pressure, $P(x)$, resulted from atmospheric pressure, P_0, and hydrostatic pressure of the riser and, counteracted by pressure drop in the interdendritic channels, is expressed as

$$P(x) = P_0 + \rho_L g h - \frac{\mu \beta V_s l}{\gamma} \int_0^x \frac{dx}{f_L(x)} \qquad [2]$$

where h is the height of the riser head. The liquid fraction is assumed to be linearly proportional to the distance from the solid interface along the x direction according to Lecomte-Beckers:[12]

$$f_L(x) = 1 - \left(\frac{x}{l}\right) \qquad [3]$$

Thus,

$$P(x) = P_0 + \rho_L g h - \frac{\mu \beta V_s l}{\gamma} \int_0^x \frac{dx}{l - x} \qquad [4]$$

$$P(x) = P_0 + \rho_L g h - \frac{\mu \beta V_s l}{\gamma} [-\ln (l - x)]_0^x \qquad [5]$$

where l is the interdendritic capillary length. There is a divergent point at $x = l$, which is physically in coincidence with the model considered by Davies,[9] who stated that the feeding problem starts in the range of 90 to 99 pct solidified melt depending on the alloys. For these reasons, a characteristic length $x = l^* < l$ is introduced to circumvent a mathematical and physical singularity. Thus, Eq. [5] yields

$$P(x) = P_0 + \rho_L g h - \frac{\mu \beta V_s l}{\gamma} \ln \frac{l}{l - l^*} \qquad [6]$$

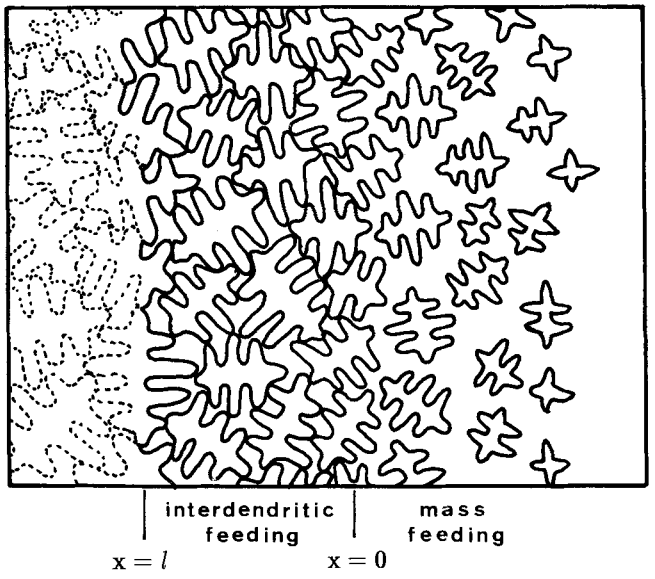

Fig. 4—Definition of capillary length for interdendritic feeding.

At $x = 0$, the pressure drop term is zero, and at $x = l^* \rightarrow l$, the pressure drop is drastically larger. Once it is overcome by the critical dissolved pressure of hydrogen, the porosity could nucleate. The l^* can approach l without porosity formation if the gas content is low enough and the heterogeneous attribution is deficient; thus, the pressure drop, denoted as "shrinkage pressure" by Campbell,[18] becomes extremely high and induces burst and solid feeding. The factor $\ln [l/(l - l^*)]$ is determined by the types of models of solidification and the critical radius of porosity, which depend on the alloying element of the melt and the hydrogen concentration of the melt, respectively. The value of $l - l^*$ is equal to the critical radius of porosity; this is identical to the feeding problem from the 90 to 99 pct fraction of solidification concluded by Davies. Thus, for a specific gas content in a melt, $\ln [l/(l - l^*)]$ is considered as a characteristic constant of this alloy. The thermal gradient, G, is introduced in Eq. [6] by the relation $G = \Delta T/l$, where ΔT is the solidification range of the alloy. Thus, the pressure drop at the root of the interdendritic channel becomes

$$P = P_0 + \rho_L g h - A \frac{\mu \beta \Delta T}{\gamma} \frac{V_s}{G} \qquad [7]$$

where $A = \ln [l/(l - l^*)]$. The generally accepted expression of γ is $\gamma = 1/(24\pi) n \tau^3$, where tortuosity, τ, can be considered as a constant for the same dendritic structure and n is the number of interdendritic channels per unit area and is inversely proportional to the square of secondary dendrite arm spacing (DAS). Equation [7] therefore becomes

$$P = P_0 + \rho_L g h - A 24 \pi \tau^3 \mu \beta \Delta T \left(\frac{1}{\mathrm{DAS}}\right)^2 \frac{V_s}{G} \qquad [8]$$

According to Flemings' work, the secondary dendrite arm spacing is proportional to local solidification time, t, by the relation $\mathrm{DAS} = Ct^{1/3}$.[19] For the present alloy studied, the C was found to be 0.042 cm when t was measured in minutes; thus,

$$P = P_0 + \rho_L g h - AB \frac{V_s}{G \cdot t^{2/3}} \qquad [9]$$

where $B = 24 \pi \tau^3 C^{-2} \mu \beta \Delta T$.

B. *Nucleation and Growth of Porosity*

The hydrostatic pressure term contributed by the riser head in Eq. [9] is very small, since at the final stage of solidification, the flow of liquid in the riser is also interdendritically viscous, as postulated by Liu *et al.*[5,6] Thus, the local pressure is negative, *i.e.*, much smaller than the atmospheric pressure in effect. Once the pores nucleate under the negative pressure, they start to grow in the interconnected interdendritic space to compensate for the solidification shrinkage and become porosity. The final volume of porosity is related to the supersaturated mass of hydrogen in liquid phase. If the hydrogen content in the melt is m mole, the volume of porosity, V_p, can be determined by local pressure:

$$V_p = mRT/P \qquad [10]$$

where R is the gas constant. Inserting the local pressure expressed by Eq. [10] in Eq. [9] yields

$$V_p = mRT \frac{1}{(P_0 + \rho_L gh - ABV_s/G \cdot t^{2/3})} \quad [11]$$

It is apparent that the volume of porosity decreases not only with increasing thermal gradient but also with decreasing solidus velocity. Consequently, the integrated term $(G \cdot t^{2/3})/V_s$ can be defined as the feeding efficiency parameter to predict the formation of porosity.

IV. RESULTS AND DISCUSSION

X-ray photographs of castings along the longitudinal center cross section reveal two kinds of microcavities, *i.e.*, the surface puncture pinhole and the internal porosity, as shown in Figure 5. In this figure, castings with a riser size of 0 to 11 cm in diameter from top to bottom are exhibited. The castings with or without small risers contain macroshrinkage cluster; increasing riser size eliminates the cluster and leaves only dispersed porosity visible. Further increasing the riser size can further reduce the dispersed porosity.

The distributions of porosity within the casting are shown in Figure 6. This figure shows that the amount of porosity is lower at the free end; it gradually increases to a maximum and then decreases again toward the riser. There are two interesting phenomena observed in Figure 6. First, there is an unexpected porosity minimum adjacent

(*a*)

(*b*)

Fig. 5—Longitudinal center cross section of castings examined by X-ray showing shrinkage cavity and porosity: (*a*) L = 15 cm castings and (*b*) L = 25 cm castings. The digits are riser diameters in centimeters.

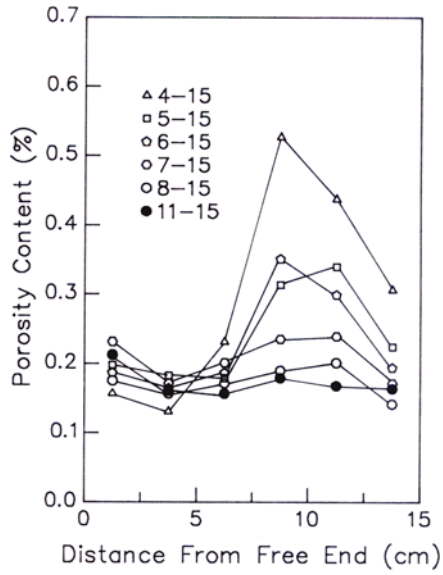

(*a*)

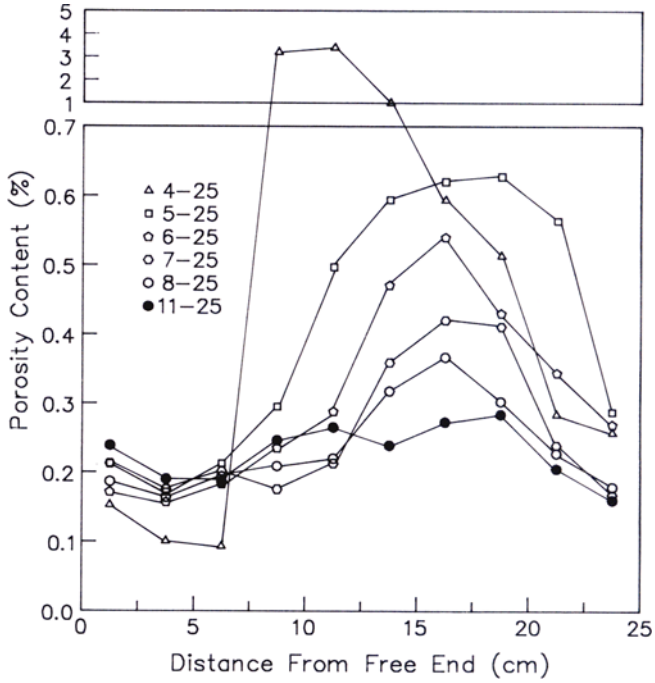

(*b*)

Fig. 6—Distribution of porosity of (*a*) L = 15 cm castings and (*b*) L = 25 cm castings.

to the free end. The free end, with three surfaces dissipating heat to the mold, acts as a chill which provides good feeding conditions for the local position adjacent to it. Second, the porosity level at the free end of the smallest risered castings (*e.g.*, 4-15, 4-25) is unexpectedly lower than other castings. These castings, as shown in Figure 5, also suffer from macroshrinkage clusters. Development of macroshrinkage obviously releases the buildup of negative hydrostatic pressure,[18] which has rendered the porosity of these castings at the free end unexpectedly lower.

A. *Effect of Casting Geometry on Thermal Parameter*

Solidification diagrams shown in Figures 7(a) and (b) exhibit the effect of length of casting and riser size on local solidification time. The local solidification time near the riser end is significantly increased, while the corresponding solidus velocity is much reduced by increasing riser diameter and the length of casting exerts little effect on them near the riser.

The variation of thermal gradient with riser size, casting length, and location in castings is shown in Figure 8. The thermal gradient is lowest at about the middle position of the casting, its value being larger both at the free end and riser end. Not only increasing the solidification time of the riser but also decreasing the length of casting can achieve a higher thermal gradient.

The motion of solidus in a solidifying casting, termed "solidus velocity," is shown in Figure 9. Solidus velocity is low at the free end; it then increases to a maximum at about 1/3 position from the riser end and finally decreases at the riser end. The advance of solidus velocity in short casting is slower than that in longer casting, and it is also reduced by increasing riser diameter.

B. *Feeding Efficiency Parameter*

The thermal gradient is a simple and good feeding efficiency parameter which has been widely used to predict the formation of porosity. Physically, it relates to

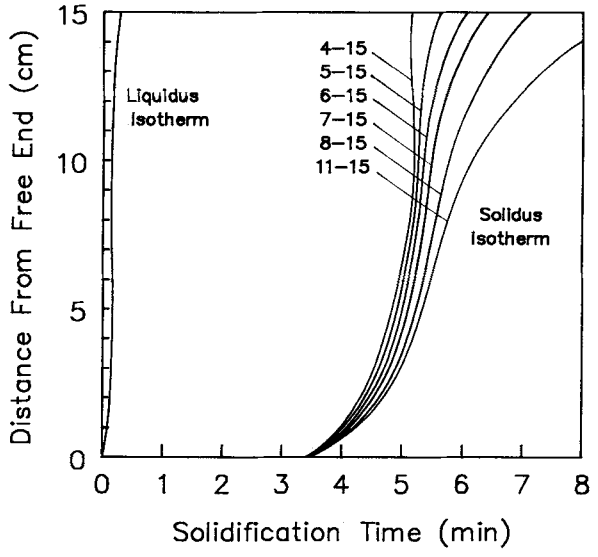

(*a*)

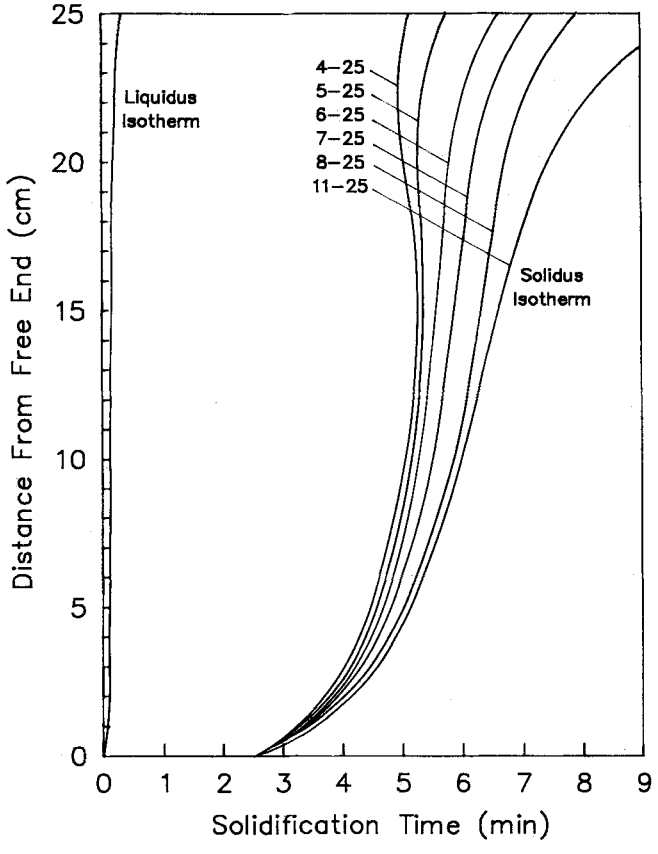

(*b*)

Fig. 7—Solidification diagram of (*a*) L = 15 cm castings and (*b*) L = 25 cm castings.

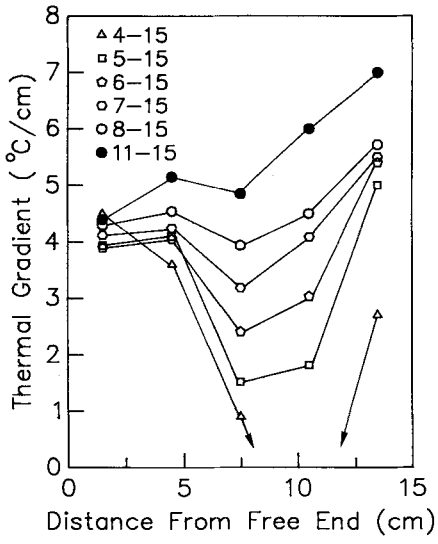

(*a*)

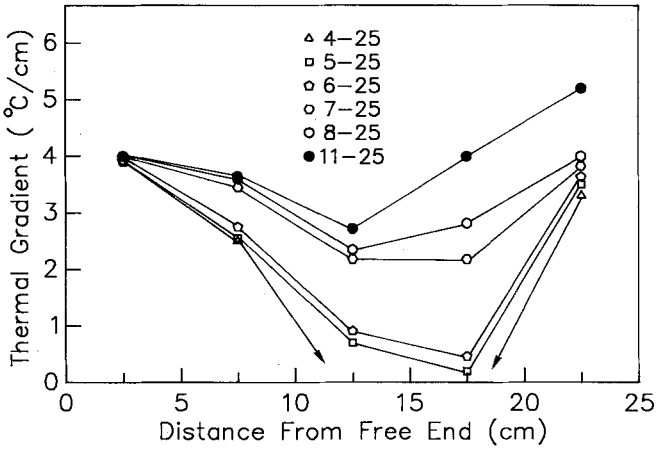

(*b*)

Fig. 8—Variation of thermal gradient in (*a*) L = 15 cm castings and (*b*) L = 25 cm castings.

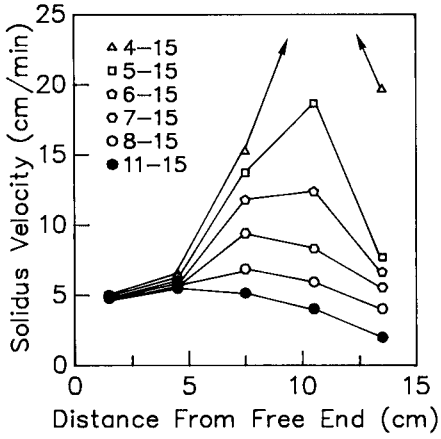

(*a*)

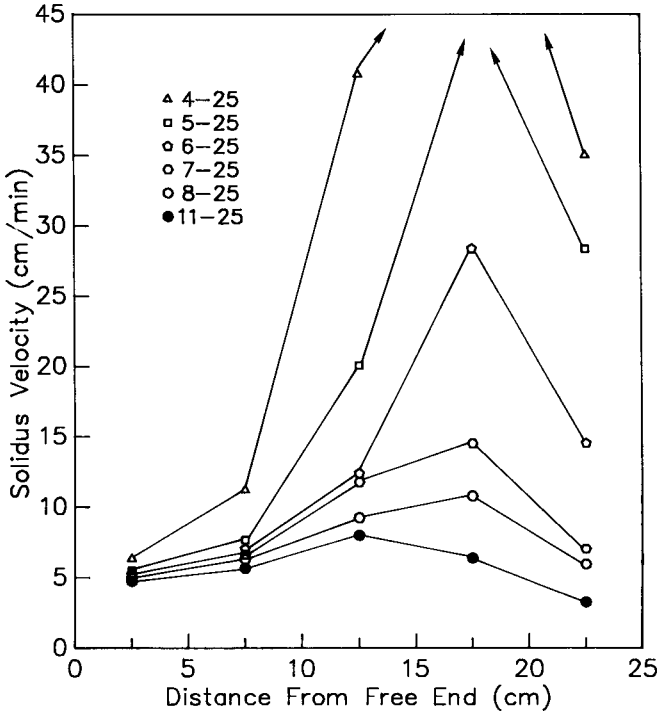

(*b*)

Fig. 9—Motion of solidus in (*a*) L = 15 cm castings and (*b*) L = 25 cm castings.

the length of the capillary interdendritic feeding channel through the relation $G = G_L \cdot \Delta T$, where G_L is the liquid fraction gradient. Since the thermal gradient is inversely proportional to the length of the capillary interdendritic feeding channel, a high thermal gradient results in a shorter capillary feeding channel and reduces the pressure drop which rose by interdendritic viscous flow, in accordance with Eq. [11]. The individual effect of local thermal gradient on the corresponding porosity content of all of the castings investigated is shown in Figure 10. As shown in this figure, the scatter in experimental results is rather large, acknowledging the errors in measurement. This parameter *per se* appears to be unable to account for all of the variables involved in describing the feeding behavior of Al-7Si-0.3Mg alloy.

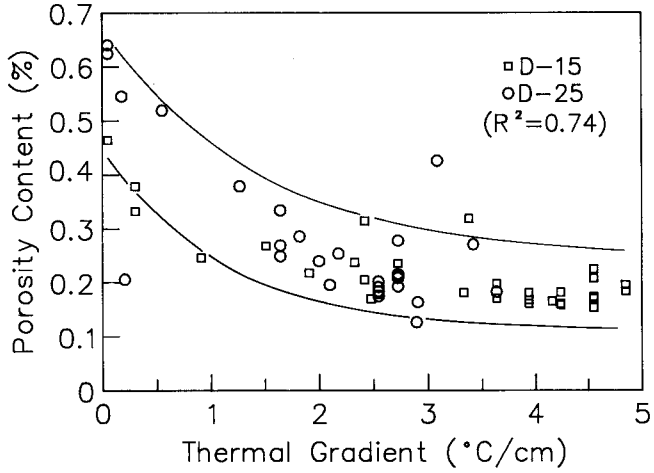

Fig. 10—Relation of thermal gradient and porosity content (where R^2 is square of multiple correlation coefficient).

The importance of solidus velocity, which had been theoretically calculated by Davies[9] according to the Hagen-Poiseuill equation, is modified into the present model based on the similar Darcy's law and substantiated by experimental measurements. The individual relation between solidus velocity and porosity content is shown in Figure 11; high solidus velocity means that a large amount of capillary fluid flow at a shorter time is required to compensate for the solidification shrinkage where the law of mass conservation still persists. In another point of view, the higher the velocity of the liquid/solid interface sweeping from free end to feeder end through a solidifying casting, the less will be the time available for interdendritic feeding.

Solidification time has also been proposed as an important factor on porosity formation and supported by experimental results in the literature.[15,16] A feeding efficiency index, defined as the ratio of thermal gradient to solidification time, G/t, without theoretical justification has been proposed to be best fitting for tensile strength data of Al-Cu-Si (LM4) alloy.[20] The generally

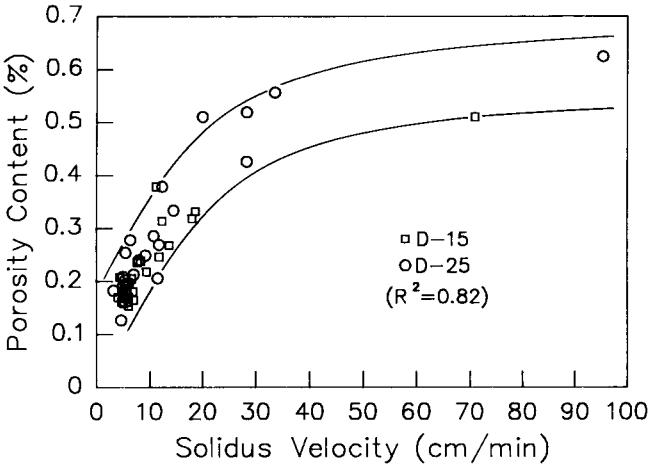

Fig. 11—Relation of solidus velocity and porosity content (where R^2 is square of multiple correlation coefficient).

accepted concept is that solidification shrinkage is reduced by increasing solidification rate. But this result contradicts feeding theory based on Darcy's law. The permeability of dendritic network for capillary fluid flow increases with increasing dendrite arm spacing, which is proportional to solidification time.[4,7] The porosity content plotted as a function of feeding efficiency index, G/t, is shown in Figure 12; however, the scatter this index experienced is still rather considerable.

It is doubtful whether solidification time alone can be considered as an independent thermal variable to characterize the feeding problem of a solidifying casting, since process variations which change t will always bring about the concurrent change in other related thermal variables. For this reason, the individual effect of t on the feeding will become unambiguous if a relation of porosity content *vs* time can be plotted while keeping all related variables constant. The relation between porosity content and solidification time plotted at iso-G/V_s ratio is shown in Figure 13. The justification of measuring t at constant G/V_s is based on the theoretical derivation of Eq. [11].

As shown in Figure 13, the relation between porosity content and solidification time appears to be categorized into two regimes, as partitioned by the dotted line. At the lower solidification time regime (denoted as regime I), the porosity content increases with increasing time, whereas at the higher solidification time regime (denoted as regime II), the porosity content decreases with increasing time. Maxima of porosity content are observed at medium solidification time, especially at lower iso-G/V_s lines where the feeding becomes unfavorable. At higher G/V_s values, *i.e.*, under good feeding conditions, the measured porosity content appears to be less affected by the solidification time. The increasing tendency of porosity with solidification time in regime I is proven to be nonrelevant to improved mass feeding because of higher solidification rate, as postulated by Davies,[9] since Chang and Chou[21] have shown that a large variation of grain size (effected by changing the inoculant content) in IN-713LC superalloy exerts insignificant variation of porosity content. The relation in regime I is attributed to one of the following growth-controlled mechanisms: (1) reduced hydrogen diffusion

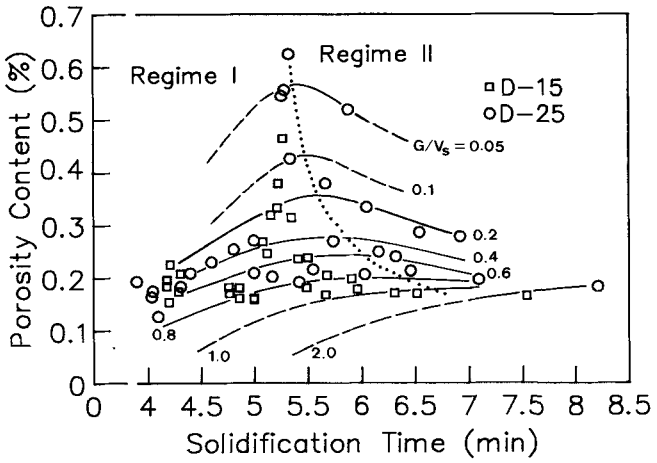

Fig. 13—Porosity content as a function of solidification time.

to the nucleated void or (2) reduced size of solidification structure[13–15,17] because of higher solidification rate.

In regime II, this phenomenon can be well accounted by Darcy's law, as has been described in this paper and in the literature;[9–12] briefly, in this regime, the porosity content is reduced by the high permeability of the coarser dendritic structure which facilitates the interdendritic feeding. This is particularly applicable for the present case of Al-7Si-0.3Mg alloy with a long period of eutectic reaction during solidification. Thus, Darcy's law, which has been advocated by many workers in attempts to quantify the feeding behavior of long freezing range alloys, is only applicable to certain thermal conditions in a solidifying casting.

A new feeding efficiency parameter integrating all individual thermal variables, denoted as $(G \cdot t^{2/3})/V_s$, is derived. Acknowledging the limitation imposed on Darcy's law as discussed above, the prediction of porosity formation by this index is shown in Figure 14. Regardless of the variation in casting geometries, the porosity content of all castings studied is satisfactorily predicted over a wide range of variables considered by this new interdendritic feeding efficiency parameter.

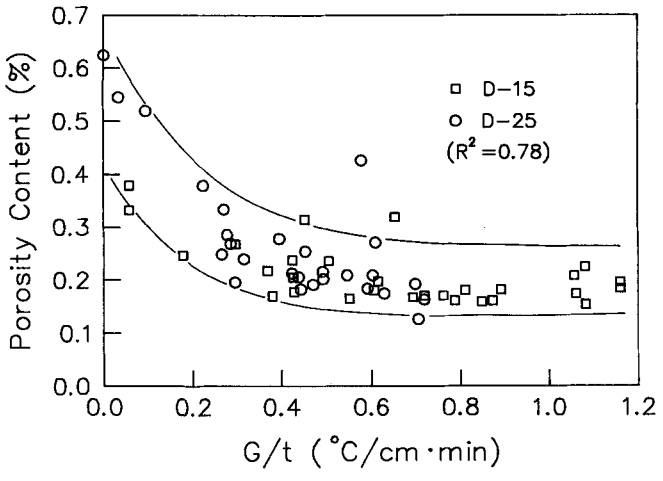

Fig. 12—Porosity content as a function of index, G/t.

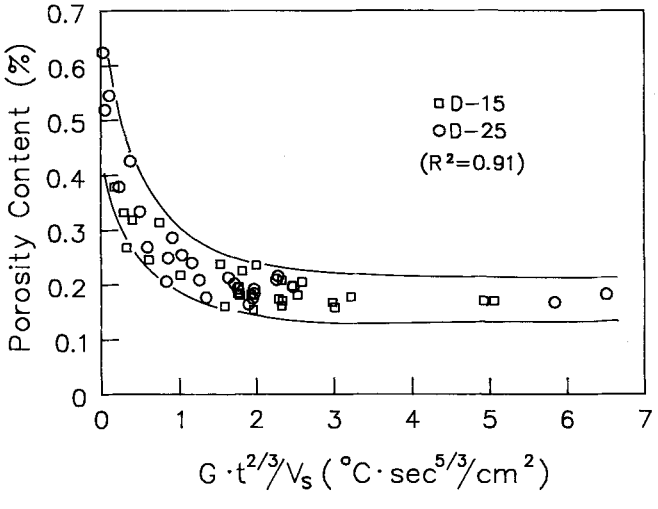

Fig. 14—Prediction of porosity by feeding efficiency parameter.

V. CONCLUSIONS

1. Darcy's law, which has been suggested to govern the interdendritic fluid flow of the porous media, is only applicable to certain thermal conditions in modeling the solidifying casting of Al-7Si-0.3Mg alloy.
2. Solidification time alone cannot be considered as an independent thermal variable to characterize the feeding behavior of a casting. At regime I, the porosity content increases with increasing solidification time, whereas at regime II, the porosity content decreases with increasing solidification time.
3. A new feeding efficiency parameter integrating all individual thermal variables, denoted as $(G \cdot t^{2/3})/V_s$, is found satisfactory to predict the formation of porosity in Al-7Si-0.3Mg castings.
4. Combined geometries of a casting and its riser size exert a great influence on the thermal variables of the Al-7Si-0.3Mg alloy in a complicated way. Together, these thermal variables synergize to govern the feeding behavior of the casting.

REFERENCES

1. T.S. Piwonka and M.C. Flemings: *Trans. TMS-AIME*, 1966, vol. 236, pp. 1157-65.
2. D. Apelian, M.C. Flemings, and R. Mehrabian: *Metall. Trans.*, 1974, vol. 5, pp. 2533-37.
3. K. Murakami and T. Okamoto: *Acta Metall.*, 1984, vol. 32, pp. 1741-44.
4. K. Murakami, A. Shiraishi, and T. Okamoto: *Acta Metall.*, 1984, vol. 32, pp. 1423-28.
5. C.Y. Liu, K. Murakami, and T. Okamoto: *Acta Metall.*, 1986, vol. 34, pp. 159-66.
6. C.Y. Liu, K. Murakami, and T. Okamoto: *Acta Metall.*, 1986, vol. 34, pp. 1173-78.
7. D.R. Poirier: *Metall. Trans. B*, 1987, vol. 18B, pp. 245-55.
8. M.C. Flemings: *Solidification Processing*, McGraw-Hill, Inc., New York, NY, 1974, pp. 234-39.
9. V. de L. Davies: *AFS Cast Met. Res. J.*, June, 1975, vol. 11, pp. 33-44.
10. E. Niyama, T. Uchida, M. Morikawa, and S. Saito: in *49th Int. Foundry Congress*, 1982, pp. 1-12.
11. S. Minakawa, I.V. Samarasekera, and F. Weinberg: *Metall. Trans. B*, 1985, vol. 16B, pp. 823-29.
12. J. Lecomte-Beckers: *Metall. Trans. A*, 1988, vol. 19A, pp. 2341-48.
13. D.R. Poirier, K. Yeum, and A.L. Maples: *Metall. Trans. A*, 1987, vol. 18A, pp. 1979-87.
14. K. Kubo and R. D. Pehlke: *Metall. Trans. B*, 1985, vol. 16B, pp. 359-66.
15. R.A. Entwistle, J.E. Gruzleski, and P.M. Thomas: in *Solidification and Casting of Metals*, The Metals Society, London, 1979, pp. 345-49.
16. S.D. Pathak and O. Prabhakar: *AFS Trans.*, 1984, vol. 92, pp. 671-80.
17. E. Bachelet and G. Lesoult: in *High Temperature Alloys for Gas Turbines*, Applied Science Publishers, Ltd., Barking, Essex, United Kingdom, 1978, pp. 665-97.
18. J. Campbell: *AFS Cast Met. Res. J.*, Mar., 1969, vol. 5, pp. 1-8.
19. M.C. Flemings: *Solidification Processing*, McGraw-Hill, Inc., New York, NY, 1974, pp. 146-48.
20. G.V. Kutumba Roa and V. Panchanathan: *AFS Trans.*, 1973, vol. 81, pp. 110-14.
21. E. Chang and J.C. Chou: *AFS Trans.*, 1987, vol. 95, pp. 749-54.